RSC Advances

COMMUNICATION

View Article Online
View Journal | View Issue

Cite this: *RSC Adv.*, 2016, **6**, 98243

Electrochemical preparation of tin–titania nanocomposite arrays†

D. Prutsch,[a] M. Wilkening[ab] and I. Hanzu*[ab]

Received 29th July 2016
Accepted 10th October 2016

DOI: 10.1039/c6ra19209b

www.rsc.org/advances

We report the first successful electrodeposition of Sn inside self-organized anodic titania nanotubes. Several relevant electrochemical parameters are identified and mechanistic aspects are briefly discussed. It appears that the role of the substrate is complex, titania acting as a mediator for Sn electrodeposition.

Introduction

Over the last decades, one-dimensional nanostructured materials, such as nanowires, nanofibers, nanorods and nanotubes have attracted significant attention following the combination of size, shape and exciting physical and chemical properties. The synthesis of transition metal oxide nanostructures with controlled dimensions and chemical composition is today of major importance, opening unmatched opportunities towards photochemical, electronic, biomedical and environmental applications. In particular, self-assembled, highly parallel TiO_2 nanotubes fabricated by anodization (*i.e.* electrochemical oxidation) of titanium have attracted significant interest in the past decade.[1] These nanotubular structures, that usually feature a relatively large surface area and a well defined geometry, possess a unique combination of properties such as non-toxicity, good chemical and mechanical stability, high oxidative power, resistance to corrosion, photocatalytic activity, environment-friendliness and even biocompatibility. These outstanding features resulted in a continuously expanding panel of proven applications including self-cleaning coatings,[2] solar cells,[3] gas sensing,[4] switching electrochromic devices,[5] rechargeable batteries,[6] electrocatalysis,[7] photocatalysis[8] and biomedical applications.[9]

Moreover, due to their highly ordered nanotubular structure, TiO_2 nanotubes can serve as an excellent substrate for further loading with a second functional material such as metals (*e.g.*, Ni, Ag, Pt)[10–12] or semiconductors (*e.g.*, CdS, $ZnFe_2O_4$, Cu_2O)[13–15] resulting in tubes with either enhanced or completely new properties. Yang *et al.*[16] found out that filling of the nanotubes with Co–Ag–Pt increases the catalytic activity, while Fe_3O_4 introduces additional magnetic properties.[17] Although, so far, several approaches for the deposition of different materials into titania nanotubes have been reported, electrodeposition is probably the most cost-effective method to fill TiO_2 nanotubes. Liu *et al.*[18] already reported on the electrodeposition of some noble metals (Pt, Au, Ag) as well as Cu into anodic TiO_2 nanotubes. However, to the best of our knowledge, there is hitherto no report available that deals with the electrochemical embedding of any base metals, such as Sn, into the inner volume of the tubes. Nanostructured Sn-based materials were already demonstrated as high-capacity anodes in Li-ion[19,20] and Na-ion batteries.[21,22] Encapsulation of Sn metal is expected to prevent coalescence of Sn nanoparticles, thus ensuring a longer cycle life of the electrode.[23] Also, it is possible to convert the Sn nanostructures into SnO or SnO_2 and obtain materials with applications to solar cells,[24] sensors[25] and catalysis.[26]

Here we report, for the first time, the partial filling of highly ordered TiO_2 nanotubes with Sn metal by electrodeposition using a simple pulsed-current deposition technique. We briefly discuss on some relevant electrochemical parameters, morphology of the deposits as well as on the apparent complexity of Sn electrodeposition onto anodic titania nanotubes.

Results and discussion

As mentioned above, electrodeposition of some noble metals as well as Cu into anodic TiO_2 nanotubes was earlier reported by Liu *et al.*[18] They used a pulsed current electrodeposition approach: each short negative (reduction) current pulse (1 s) was followed by a relatively long rest period (7 s) in order to allow the electrode surface to replenish with aqueous cations by diffusion. So far, only the influences of the pulse length and the rest periods are discussed. The best conditions for electrodeposition are, however,

[a]*Institute for Chemistry and Technology of Materials, Graz University of Technology, Stremayrgasse 9, 8010 Graz, Austria. E-mail: hanzu@tugraz.at*

[b]*Christian Doppler Laboratory for Lithium Batteries, Graz University of Technology, Stremayrgasse 9, 8010 Graz, Austria*

† Electronic supplementary information (ESI) available. See DOI: 10.1039/c6ra19209b

still unclear. In general, electrodeposition on oxidic substrates is notoriously difficult to conduct[27] because numerous electrochemical parameters, whose values are initially unknown, may significantly influence the deposition process. Thus, in order to shed some light on this essential information and to quickly identify the relevant parameters that lead to filling of the titania nanotubes, the successful silver electrodeposition bath of Liu *et al.* was used as a starting point. Cyclic voltammetry experiments were carried out in a conventional 3-electrode electrochemical configuration with a glassy carbon working electrode. In the second step, the same experiments were done for the Sn-containing electrodeposition bath. The results are shown in Fig. 1.

We noticed that Ag deposit already has a visible dendritic appearance even at relatively low current densities of 3.6 mA cm^{-2} while the Sn looked significantly smoother on the surface of the glassy carbon electrode even at a current density as high as 15.4 mA cm^{-2}. Dendritic electrodeposition of metals occurs when the limiting diffusion current is exceeded, at least locally. As the surface of the electrode is depleted on cation species, inhomogeneous growth occurs. Once nucleated, the dendrites grow very fast as the electric field at their point tips is significantly higher than on the flat surface of the electrode.

Based on the report of Liu *et al.* and on our observations it appears that in order to successfully achieve the electrodeposition of a metal inside the anodic titania nanotubes it is preferable to work at high current densities, *i.e.*, above the limit of dendritic deposition. Since there were visual indications that even at a current density of 15.4 mA cm^{-2} the Sn deposit still had a smoother appearance than Ag we decided to drastically increase the current density for the pulsed electrodeposition of Sn in TiO_2 nanotubes to 1 A cm^{-2} in order to achieve the dendritic electrodeposition regime that seemed necessary. First, a short reduction pulse ($I_{on} = -1$ A cm^{-2}, $t_{on} = 0.5$ s) was applied in order to electrodeposit Sn followed by a rest period of 10 s to restore the tin concentration at the interface.

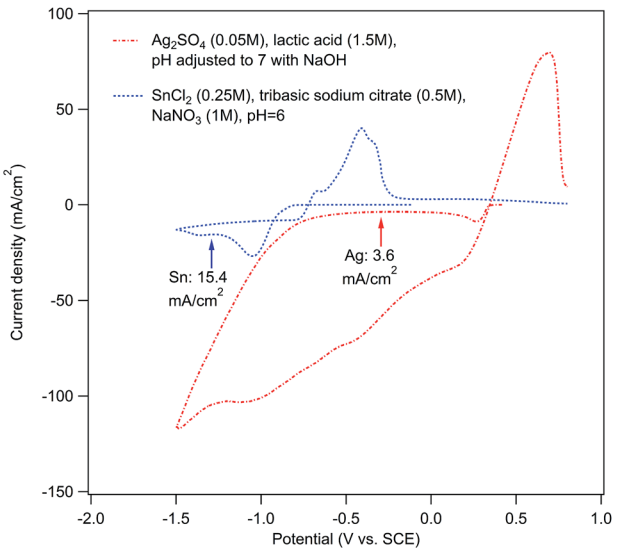

Fig. 1 Cyclic voltammograms of the electrodeposition baths for Ag and Sn at a scan rate of 25 mV s^{-1} between 0.8 V and −1.5 *vs.* SCE.

Fig. 2, left side, shows top-view (a) and cross-section (b) Scanning Electron Microscopy (SEM) images acquired using a Secondary Electrons (SE) detector. The images show the titania nanotube layer on which Sn was electrodeposited after a total of 90 current pulses according to the pulsed electrodeposition procedure described above. On the right side, the same regions are shown, however, imaged with a Back-Scattered Electrons (BSE) detector which delivers SEM micrographs featuring good chemical element contrast. The bright regions correspond to the Sn deposit. It can clearly be seen that Sn has been successfully embedded into the inner volume of the nanotubes. It is also evident that Sn is not found in all the nanotubes which means that electrodeposition does not occur in a homogeneous manner. The presence of metallic Sn was confirmed by X-ray diffraction (see ESI, Fig. S2†).

In Fig. 3 the corresponding potential response is shown. Upon the application of the reduction pulse I_{on}, the potential of titania nanotubes electrode drops to very low values of approximately −9.5 V *vs.* SCE (Saturated Calomel Electrode). Subsequently, a relatively small voltage recovery is recorded over the entire duration of the current pulse (see the inset of Fig. 3). This relative potential variation is consistent with a typical chronopotentiometric response of an electrodeposition process. The enormous potential drop to −9.5 V can be explained by the relatively low electronic conductivity of the initial TiO_2 nanotubes[28] that lead to high ohmic drops. This assumption is supported by the instant potential recovery to approx. −1.5 V *vs.* SCE that occurs just after the reduction current pulse. Afterwards, from −1.5 V, also a relatively fast recovery of the electrode potential was recorded; the potential effectively reaches a stable value after 6 s. Indeed, for the last 4 seconds of the rest period a variation of the electrode potential of less than 25 mV has been found. This fast relaxation behaviour may be explained if we consider the stirring effect generated by the significant hydrogen evolution at the electrode which leave only small concentration gradients in the electrodeposition bath at the end of the current pulse.

If we consider that at the beginning the electronic conductivity of anodic titania nanotubes is low, the preferred place for the nucleation and grow of Sn should be at the bottom of the nanotubes. This expectation is, however, not supported by observation. In fact, the Sn appears to nucleate and grow from the top towards the inner volume of the nanotubes (see ESI, Fig. S1†). This intriguing behaviour is an indication of a fundamentally different electrodeposition mechanism. Indeed, it is known that it is possible to reduce TiO_2 in aqueous media and insert a significant amount of protons in TiO_2 nanotubes.[29,30] The Ti^{3+} centres formed are, however, not stable in aqueous media and Ti^{3+} re-oxidizes completely within minutes back to Ti^{4+}. It is then plausible to assume that the deposition of Sn inside the nanotubes might occur according to the following mechanism. First, the high current pulse reduces TiO_2 to H_xTiO_2. Since the Ti^{3+} state is not stable, it is likely that during the rest period Sn^{2+} is in fact reduced by the re-oxidation of H_xTiO_2, thus, leading to the slow growth of Sn in the nanotubes with the nucleation point at the top of the nanotubes rather than at the bottom. Thus the high current reduction

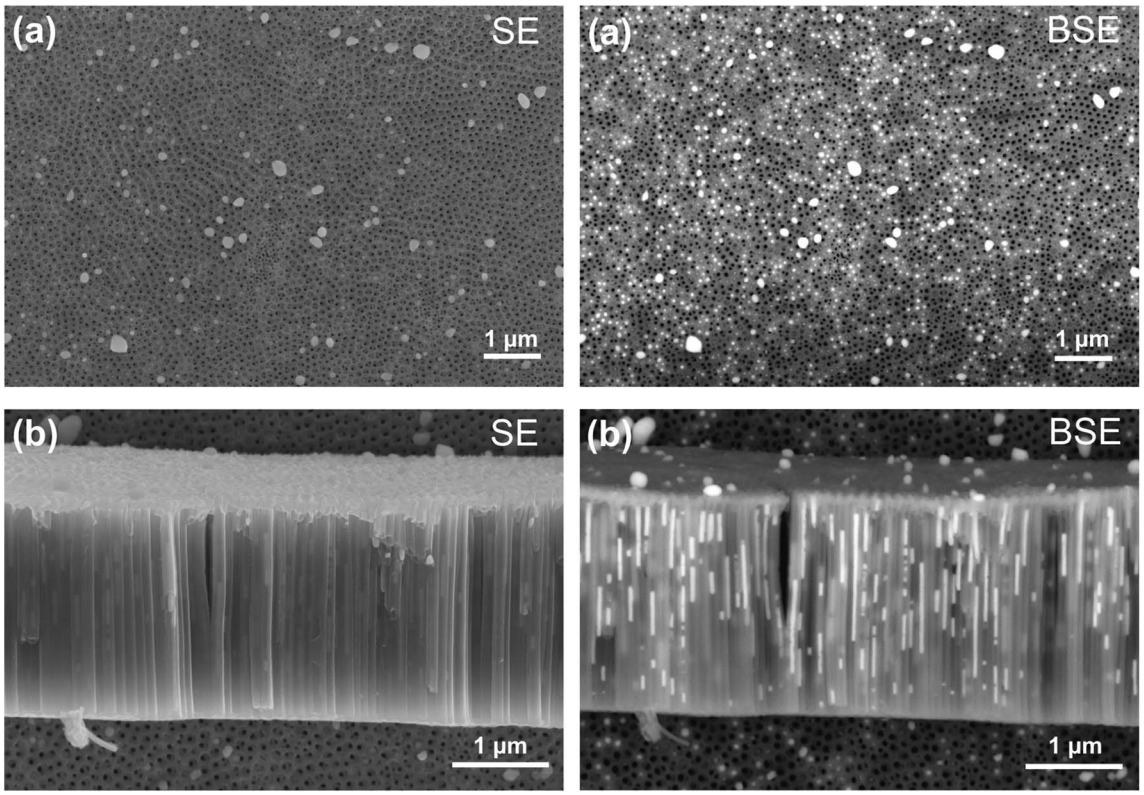

Fig. 2 Left: Secondary Electrons (SE) SEM images in top-view (a) and cross-section (b) of a TiO_2 nanotube layer on which Sn has been deposited using a pulsed electrodeposition technique. Right: The same regions imaged with a Back-Scattered Electrons (BSE) detector showing an improved chemical composition contrast. It is obvious that Sn is indeed embedded inside the nanotubes. See text for further discussion of the deposition mechanism.

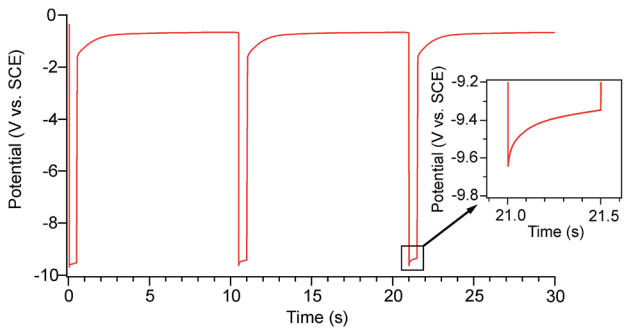

Fig. 3 Chronopotentiometric curves recorded during the pulsed Sn electrodeposition on anodic TiO_2 nanotubes. See text for further explanation.

pulses might not directly lead to the Sn growth inside the nanotubes but to the germination of Sn crystallites. These crystallites may subsequently act as seeds for the relatively slow growing of Sn during the rest periods. Obviously, according to this scenario only the germs that have access to a sufficient Sn^{2+} flux will grow. The germs closer to the open top of the nanotubes will grow while those at the bottom will never develop further. With each reduction pulse the Ti^{3+} reserve is replenished and Sn growth inside the nanotubes continues, at points where Sn^{2+} is available. In the case of electrodeposition, the nucleation of Sn on titania nanotubes substrates is instantaneous,[31] *i.e.* all tin germs form at the beginning upon the application of the current, with only growth of the germs occurring thereafter. Since the rest period during the reduction pulses is relatively long, each reduction pulse will also generate new Sn germs within the nanotube layer. Consequently, there is a direct dependence of the nanotube filling ratio on the number of pulses applied (see ESI, Fig. S1†). This mechanism could explain satisfactorily the wide distribution of the Sn deposits length inside the nanotubes, as is clearly seen in Fig. 2. Hence, the distribution width is a natural consequence of the variable access to aqueous tin species as well as the different moment at which the tin germs form and start growing.

Conclusions

We report, for the first time, the electrodeposition of Sn inside anodic titania nanotubes by using a high-current density pulsed electrodeposition method. While at first sight, it appeared that dendritic electrodeposition is required to embed metals within the inner volume of the nanotubes, the mechanism in the present case seems to be quite different from that of classical electrodeposition. It turned out that the growth of Sn inside the nanotubes is much more complex than expected. We suggest that it occurs through an indirect, redox-mediated mechanism

in which the titania substrate most likely plays the role of redox mediator. This could in fact constitute a more general route, opening the way for the facile realization of highly regular titania-base metal nanocomposites by easily practicable electrochemical means.

Experimental

The Ag electrodeposition bath reported by Liu *et al.* (containing 0.05 M Ag_2SO_4, 1.5 M lactic acid; the pH was adjusted to 7 with NaOH) was prepared and cyclic voltammetry experiments were carried out in a classical three-electrode configuration with a glassy carbon working electrode, a platinum gauze counter electrode and a Saturated Calomel Electrode (SCE) in a Haber–Luggin capillary that served as a reference electrode. Cyclic voltammograms were recorded between −1.5 V and 0.8 V at scan rates of 25 and 50 mV s^{-1} using a Parstat MC potentiostat running Versa Studio software. The same experiments were done for a Sn deposition solution consisting of $SnCl_2$ (0.25 M), tribasic sodium citrate (0.5 M) and $NaNO_3$ (1 M), whose natural pH = 6. For the preparation of the electrodeposition baths de-ionized water (Millipore) was used. All experiments were carried out at room temperature.

Titanium foils (99.7% purity, 0.25 mm thickness, Sigma Aldrich) cut in small pieces of 12.5 mm × 12.5 mm were ultrasonically cleaned in acetone, isopropanol and methanol for 10 minutes, in this order, followed by rinsing with distilled water and drying with compressed air. A two-electrode electrochemical cell with the titanium substrate as working electrode and a stainless steel counter electrode was used to perform the anodic growth of the TiO_2 nanotubes. In this cell, the sample was pressed against a brass ring in order to ensure a good electrical contact, while leaving a surface area of approx. 0.708 cm^2 of the titanium substrate exposed to the anodization bath. The electrolyte used consisted of 97.6 wt% ethylene glycol, 2 wt% distilled water and 0.4 wt% NH_4F. The electrodes were connected to a precision DC power supply (Agilent E3610A) and anodization was carried out at a constant voltage of 60 V for 1 h. The as-anodized samples were then rinsed with distilled water and dried with compressed air. In order to achieve an ordered and highly-regular tube morphology a second anodization step was applied. For this, the first nanotube layer was removed from the titanium substrate by using an adhesive scotch tape and on the same titanium substrate, after ultrasonically cleaning in acetone, isopropanol and methanol for 10 minutes, subsequent rinsing with distilled water and drying with compressed air, TiO_2 nanotubes were grown under same conditions for 5 minutes. The ordered dimples that cover the titanium substrate after peeling off the nanotube layer are acting here as nucleation sites for the titania nanotube growth in the second step. To form an oxide sealing layer underneath the titania nanotubes the samples were anodized again in a solution of 0.2 M H_3PO_4 in ethylene glycol at 20 V for 10 min in a two electrode system with a stainless steel counter electrode. Finally the as-prepared samples were rinsed with distilled water and dried with compressed air.

Partial filling of the TiO_2 nanotubes was accomplished by using a pulsed galvanostatic method. The electrodeposition experiments were carried out in a classical three-electrode configuration with the nanotube layer on the titanium substrates as working electrode, a platinum gauze as counter electrode and a Saturated Calomel Electrode as reference. The samples were fit in the same electrochemical cell that was already used for the anodization process, so that only the nanotube layer (an area of 0.708 cm^2) on the titanium substrate was exposed to the Sn deposition solution. The electrolyte for the electrodeposition of Sn metal was a mixture of $SnCl_2$ (0.25 M), tribasic sodium citrate (0.5 M) and $NaNO_3$ (1 M), pH 6. All solutions were prepared with de-ionized water (Millipore). For Sn deposition a current pulsing approach with a short pulse of negative current ($I_{on} = -1$ A cm^{-2}, $t_{on} = 0.5$ s), followed by a delay time ($I_{off} = 0$ A cm^{-2}) of $t_{off} = 10$ s was used. Different number of pulses (2, 5, 10, 20 and 90) was applied in order to follow the degree of tube filling. All electrodeposition experiments were performed at room temperature using a multichannel VMP-3 potentiostat equipped with a 20 A current booster kit from Biologic Science Instruments running EC-LAB-software (v.10.34). After Sn deposition the samples were rinsed with Millipore de-ionized water and carefully dried with compressed air. Scanning Electron Microscopy (Zeiss Ultra 55 and Vega Tescan) was employed for the morphological characterization of the filled TiO_2 nanotubes. SEM cross-section images were taken from samples that were scratched just before placing them in the SEM vacuum chamber.

Acknowledgements

Sanja Simic from Austrian Centre for Electron Microscopy and Nanoanalysis (FELMI-ZFE) is kindly acknowledged for the SEM micrographs. We also thank Brigitte Bitschnau from Institute of Physical and Theoretical Chemistry (PTC) for XRD measurements. Financial support by the Austrian Federal Ministry of Science, Research and Economy, and the Austrian National Foundation for Research, Technology and Development is greatly appreciated. Furthermore, we kindly acknowledge the Austrian Research Promotion Agency (FFG) through the RSA-AIMS project, Grant No. 4338751, as well as the Deutsche Forschungsgemeinschaft (DFG) through the Research Unit 1277 (molife), Grant No. WI 3600/4-2 and HA 6996/1-2, for financial support.

References

1 S. Berger, R. Hahn, P. Roy and P. Schmuki, *Phys. Status Solidi B*, 2010, **247**, 2424–2435.
2 R. Wang, K. Hashimoto, A. Fujishima, M. Chikuni, E. Kojima, A. Kitamura, M. Shimohigoshi and T. Watanabe, *Adv. Mater.*, 1998, **10**, 135–138.
3 J. M. Macák, H. Tsuchiya, A. Ghicov and P. Schmuki, *Electrochem. Commun.*, 2005, **7**, 1133–1137.
4 M. Paulose, O. K. Varghese, G. K. Mor, C. A. Grimes and K. G. Ong, *Nanotechnology*, 2006, **17**, 398–402.

5 A. Ghicov, H. Tsuchiya, R. Hahn, J. M. Macak, A. G. Muñoz and P. Schmuki, *Electrochem. Commun.*, 2006, **8**, 528–532.
6 D. Prutsch, M. Wilkening and I. Hanzu, *ACS Appl. Mater. Interfaces*, 2015, **7**, 25757–25769.
7 J. M. Macak, F. Schmidt-Stein and P. Schmuki, *Electrochem. Commun.*, 2007, **9**, 1783–1787.
8 A. L. Linsebigler, G. Lu and J. T. Yates, *Chem. Rev.*, 1995, **95**, 735–758.
9 S. H. Oh, R. R. Finones, C. Daraio, L. H. Chen and S. Jin, *Biomaterials*, 2005, **26**, 4938–4943.
10 Y. Zhang, Y. Yang, P. Xiao, X. Zhang, L. Lu and L. Li, *Mater. Lett.*, 2009, **63**, 2429–2431.
11 K. Xie, L. Sun, C. Wang, Y. Lai, M. Wang, H. Chen and C. Lin, *Electrochim. Acta*, 2010, **55**, 7211–7218.
12 Y.-Y. Song, Z.-D. Gao and P. Schmuki, *Electrochem. Commun.*, 2011, **13**, 290–293.
13 Y.-Y. Song, Q.-L. Zhuang, C.-Y. Li, H.-F. Liu, J. Cao and Z.-D. Gao, *Electrochem. Commun.*, 2012, **16**, 44–48.
14 Y. Hou, X.-Y. Li, Q.-D. Zhao, X. Quan and G.-H. Chen, *Adv. Funct. Mater.*, 2010, **20**, 2165–2174.
15 S. Zhang, S. Zhang, F. Peng, H. Zhang, H. Liu and H. Zhao, *Electrochem. Commun.*, 2011, **13**, 861–864.
16 L. Yang, D. He, Q. Cai and C. A. Grimes, *J. Phys. Chem. C*, 2007, **111**, 8214–8217.
17 N. K. Shrestha, J. M. Macak, F. Schmidt-Stein, R. Hahn, C. T. Mierke, B. Fabry and P. Schmuki, *Angew. Chem., Int. Ed.*, 2009, **48**, 969–972.
18 N. Liu, K. Lee and P. Schmuki, *Angew. Chem., Int. Ed.*, 2013, **52**, 12381–12384.
19 Y. M. Lin, R. K. Nagarale, K. C. Klavetter, A. Heller and C. B. Mullins, *J. Mater. Chem.*, 2012, **22**, 11134–11139.
20 Y. H. Xu, Q. Liu, Y. J. Zhu, Y. H. Liu, A. Langrock, M. R. Zachariah and C. S. Wang, *Nano Lett.*, 2013, **13**, 470–474.
21 D. H. Nam, T. H. Kim, K. S. Hong and H. S. Kwon, *ACS Nano*, 2014, **8**, 11824–11835.
22 H. L. Zhu, Z. Jia, Y. C. Chen, N. Weadock, J. Y. Wan, O. Vaaland, X. G. Han, T. Li and L. B. Hu, *Nano Lett.*, 2013, **13**, 3093–3100.
23 C. Wu, J. Maier and Y. Yu, *Adv. Funct. Mater.*, 2015, **25**, 3488–3496.
24 S. S. Bhande, G. A. Taur, A. V. Shaikh, O. S. Joo, M. M. Sung, R. S. Mane, A. V. Ghule and S. H. Han, *Mater. Lett.*, 2012, **79**, 29–31.
25 S. Das and V. Jayaraman, *Prog. Mater. Sci.*, 2014, **66**, 112–255.
26 Z. Y. Zhou, N. Tian, J. T. Li, I. Broadwell and S. G. Sun, *Chem. Soc. Rev.*, 2011, **40**, 4167–4185.
27 T. Djenizian, I. Hanzu, M. Eyraud and L. Santinacci, *C. R. Chim.*, 2008, **11**, 995–1003.
28 I. Hanzu, T. Djenizian and P. Knauth, *J. Phys. Chem. C*, 2011, **115**, 5989–5996.
29 I. Hanzu, T. Djenizian and P. Knauth, *Wide Bandgap Semiconductor Materials and Devices 12*, 2011, vol. 35, pp. 21–31.
30 I. Hanzu, V. Hornebecq, T. Djenizian and P. Knauth, *C. R. Chim.*, 2013, **16**, 96–102.
31 I. Hanzu, T. Djenizian, G. F. Ortiz and P. Knauth, *J. Phys. Chem. C*, 2009, **113**, 20568–20575.